

Granular disruption during explosive volcanic eruptions

Josef Dufek^{1*}, Michael Manga² and Ameet Patel²

Explosive volcanic eruptions are among the most energetic events on Earth. The hazard to surrounding populations and aviation is controlled by the concentration and size of particles that exit the volcanic vent. The size distribution of volcanic particles is thought to be determined by the initial fragmentation process^{1–4}, where bubbly magmatic mixtures transition to gas-particle flows. Here we show that collisional processes in the volcanic conduit after initial fragmentation can change the grain-size distribution of particles that leave the volcanic vent. We use experimental analysis of the breakup of natural volcanic rocks during collisions, as well as numerical simulations, to estimate the probability that particles pass through the volcanic conduit and survive intact. We find that breakup in the conduit is strongly controlled by the initial particle size and the location of the initial fragmentation: particles that measure more than 1 cm in diameter and those fragmented at great depths break up most frequently. Abundant large pumice clasts in volcanic deposits therefore imply shallow fragmentation that may be transient. In contrast, fragmentation events at depth will lead to enhanced ash production and greater atmospheric loading of long-residence, fine-grained ash.

Volcanic conduits are the locus of dramatic fluid transformations as very viscous magmas (some eight to ten orders of magnitude more viscous than water) fragment and produce a turbulent, particle-laden mixture. A variety of fragmentation mechanisms have been proposed including bubble overpressure⁵, strain-induced fragmentation^{6,7} and critical packing of bubbles⁸. Grain-size distributions of the resulting fragmented magma have been attributed to the vigour and mechanism of fragmentation, with the total grain-size distribution of eruption deposits expected to reflect this process⁹.

Owing to the confined nature of the volcanic conduit, the relatively high number density of particles following fragmentation and high-velocity conditions, volcanic conduits are likely sites for numerous high-energy impacts that may break these particles. Although comminution processes, especially in ground-hugging gravity currents, have been recognized for many years^{10–12}, little quantification has been undertaken.

Two considerations are necessary to evaluate the role of particle breakup in the volcanic conduit. First, what is the likelihood that particles break in response to a collision of specific energy? Second, how common are collisions in different energy ranges?

We carried out a series of experiments on natural volcanic clasts during short-duration collisions (Fig. 1). We also incorporated into our analysis high-energy collision experiments done on dense spheres and sintered glass spheres aimed at understanding

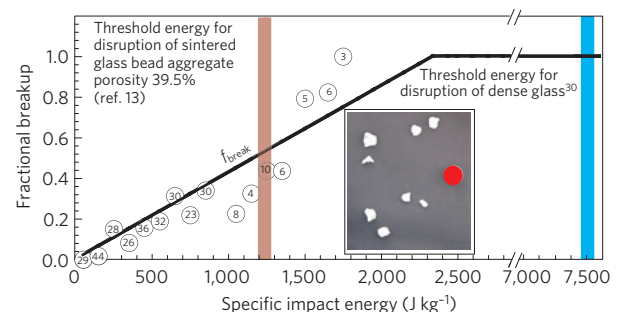


Figure 1 | Summary of pumice collision and breakup experiments. The fractions of pumice that meet the disruption criteria are plotted versus the specific impact energy (circles). The pumice experiments are plotted in 100 J kg⁻¹ energy bins, with the number of experiments in the binned range denoted in the centre of the circles. The modelled breakage threshold is plotted as a dark line ($f_{\text{break}} = A(\Delta u)^2$, where $A = 4.27 \times 10^{-4}$ and Δu is the collisional velocity). The threshold energies for disruption for sintered glass bead aggregates¹³ and dense glass³⁰ bracket the pumice results. Inset is a photograph of the products of a disruptive collision, with a reference sphere of diameter 1.27 cm (red). The disrupted clast fragments are angular and have roundness measures indistinguishable from fall deposits using a two-dimensional roundness metric.

high-velocity collisional processes during the early stages of planet formation¹³. Experiments examining the collisions of glassy, porous volcanic pumice indicate that the energy of the collision dictates the style and probability of the particles fragmenting into smaller particles. Previous experiments¹⁰ found that low-velocity impacts (<30 m s⁻¹) typically produced small fragments (<100 μm) associated with breaking bubble walls and septa. This style of fragmentation, or comminution, is probably important for the dynamics of pyroclastic density currents, that is, volcanically generated particle-laden gravity currents in which there are numerous low-energy collisions^{10,14}. At these low energies the removal of fine-ash-sized particles from pumice produces visibly rounder particles observed in many pyroclastic density current deposits^{10,15,16}.

At the higher particle collisional energies relevant for conduits¹⁷, particles begin to break into fragments that are large fractions of their initial size. These high-velocity impacts have short durations (much less than viscous relaxation timescales of magma) leading to brittle breakup similar to primary fragmentation behaviour^{5–7}. To differentiate this style of fragmentation from the production of fine fragments, we adopt the term disruption that is used commonly in the ballistic and impact experiment literature. High-energy disruptive collisions produce power law grain-size distributions and

¹School of Earth and Atmospheric Science, Georgia Institute of Technology, 311 Ferst Drive, Atlanta, Georgia 30332, USA, ²Department of Earth and Planetary Science, University of California at Berkeley, Berkeley, California 94720, USA. *e-mail: dufek@gatech.edu.

angular fragments compared with low-energy collisions. A variation in fragmentation style owing to impact energy is consistent with earlier experiments¹⁸. These showed that a power law description of grain sizes produced by the impact of a heavy piston with pumice did not change compared with the primary fragmentation distribution. However, grinding the particles in a rotating cylinder produced increased exponents up to a plateau^{15,18}.

For moderate-energy collisions (Fig. 1), not all particles will break into multiple fragments. The variability depends in part on the geometry and strength of these naturally formed pumice clasts. As the energy of the impact increases, a greater proportion of particles break into multiple macroscopic particles, until at sufficiently high energy almost all particles break into multiple large angular fragments. We note that this threshold behaviour has been observed for sintered glass beads and solid dense glass beads¹³, bracketing our current experiments (and both have the same order of magnitude of energy for disruption). Thus although we expect the behaviour and thresholds to vary between eruptions (with varying composition, crystal content and porosity) the same general trends can be expected and only the fitting constant is likely to differ. We refer to this probability as the breaking fraction, f_{break} . To determine the fraction of particles that are disrupted, the joint probability of the collisional velocity and breaking fraction needs to be evaluated.

We illustrate the key parameters in clast disruption using a simplified analytical model before considering more detailed feedbacks between disruption and flow using numerical simulations. For the analytical model we make the following assumptions, with the caveat that the more sophisticated numerical treatment is necessary to observe secondary feedback mechanisms: first, the velocity at the exit of the conduit is at the speed of sound of the dusty gas. Second, the parcel timescale can be approximated as $\tau_{\text{transit}} = L/v_{\text{centre}}$ where L is the length of the conduit and v_{centre} is the mean velocity in the centre of the conduit. Third, the dissipation of collisional granular energy is locally balanced by production owing to shear.

The amount of disruption in a collection of particles, D , is

$$D = \underbrace{\frac{144\alpha^2\sqrt{\theta}}{\pi^{3/2}d^4}}_{\text{collision rate}} \times \underbrace{ff_{\text{disrupt}}}_{\text{fraction disrupted}} \times \underbrace{\tau_{\text{transit}}}_{\text{transit timescale}} \quad (1)$$

where the fraction disrupted (ff_{disrupt}) is calculated using the experimental data integrated over collisional energies and the collision rate is determined by estimating the granular temperature, θ , (assumption 3) and considering a range of particle volume fraction, α and diameter, d . The volume fraction also contributes to the dusty gas sound speed and transit timescale (detailed development in Supplementary Methods).

Two general and important features result from this analysis: first, the number of disruptive collisions scales with the depth of fragmentation and second, disruption is sensitive to particle diameter. Two examples are illustrated in Fig. 2a,b using the material properties for pumice and dense glass and using an average volume fraction of particles of 0.05 (in a range similar to many volcanic conduit simulations)^{19–21} and a conduit diameter of 100 m.

In both the vesicular pumice example and the dense glass example the fragmentation depth and size of pumice strongly controls the number of disruptive collisions. The red shaded region of these figures shows those particle and conduit parameters that are likely to result in disruption. An important consequence of this calculation is that large pumice particles (>5 cm) are difficult to preserve unless the fragmentation depth is very shallow. Although increasing the conduit diameter reduces the predicted number of disruptive events, the limited range of expected conduit diameters, relative to variability in fragmentation depth, restricts its potential impact. For example, for a set fragmentation depth of 5,000 m,

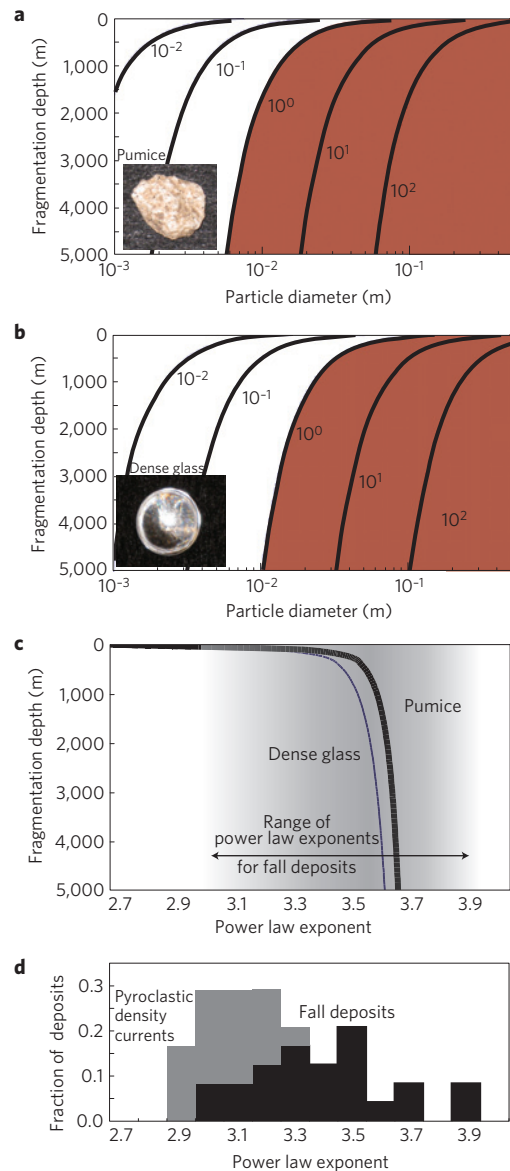


Figure 2 | Analytical model results. The contours show the number of disruptive collisions, with the shaded red region showing conditions where at least one disruptive collision is expected. **a**, Properties from pumice experiments and **b**, properties of dense glass³⁰. **c**, The power law exponent for the grain-size distribution resulting from the modelled disruptive collisions. The shaded region represents the range of power law exponents from fall deposits. **d**, The distribution of power law exponents in deposits from the data compilation of ref. 18.

increasing the conduit diameter to 200 m from 100 m results in greater than one disruptive collision for particles larger than ~2 cm compared with ~5 mm, respectively. The total grain-size distribution can also be calculated with this model (Fig. 2c), using a power law description of the size distribution, $N = \lambda r^{-D}$, where N is the number of particles greater than size r , λ is a scaling factor and D is the power law exponent. The power law exponent increases with increasing fragmentation depth. The predicted power law exponents span much of the range recorded in fall deposits (Fig. 2d) consistent with modification of the grain-size distribution following the primary fragmentation event¹⁸.

Owing to feedback in viscosity, collision rate and evolving grain sizes as a result of collisions, we expect volcanic conduits to exhibit spatial and temporal variability that could produce different

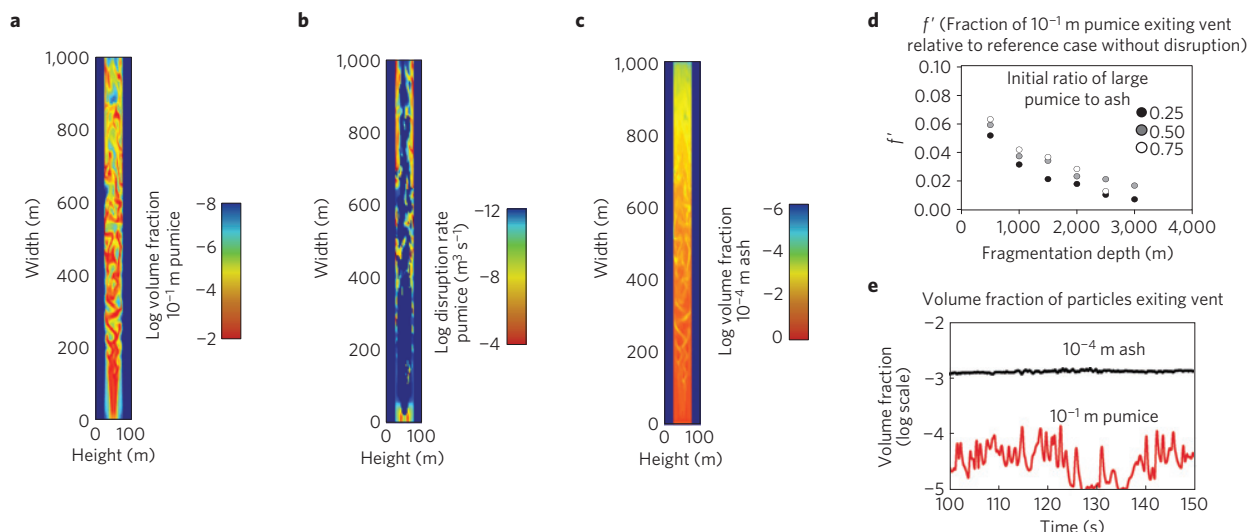


Figure 3 | Numerical simulation of particle breakup in the conduit. **a–c**, A snapshot at 100 s for a conduit of width 50 m and height 1 km. **a**, The volume fraction of 10 cm pumice; **b**, the instantaneous disruption rate; and **c**, the volume fraction of 100 μm ash. Note different scales. **d**, A summary of the fraction of 10 cm pumice that exits the volcanic vent normalized to simulations in which no collisional breakup is considered for a range of conduit depths. These fractions are averaged over 300 s of simulated time. The different colour circles express the initial pumice to ash ratio in the simulation. **e**, An example time series of ash and pumice discharge from the vent for the 1 km conduit depth simulation.

features to those predicted from the simplified analytical treatment. To examine these feedbacks we employed a multiphase numerical model using an Eulerian–Eulerian–Lagrangian framework^{22,23} (Supplementary Methods).

We considered several initial particle-size distributions in the continuum model to evaluate the sensitivity of fragmentation efficiency on particle collisions and disruption. An example simulation is shown in Fig. 3 for a fragmentation depth of 1 km. The conduit margins, where energetic collisions are most common, produce the most vigorous rates of pumice breakup. In these transient simulations the particle concentration of large pumice is heterogeneous, reflecting a granular instability whereby particles in dilute regions travel faster than those in dense regions owing to more numerous particle collisions and greater effective granular viscosity¹⁷. The concentration of fine particles is much more evenly distributed as they more closely follow the gas velocity field, although mesoscale structure still persists. This mesoscale structure leads to pulsating conditions (Fig. 3) at the conduit exit even though conditions at the fragmentation level are held steady with time.

For a range of initial particle sizes, the fragmentation depth plays the most important role in determining the fraction of large pumice that survives to be injected into the atmosphere (Fig. 3d). This confirms the main observations from the analytical model even though these simulations have time-dependent dynamics and an evolving distribution of particle sizes. When compared with simulations that do not include granular disruption, fragmentation depths of 3 km result in less than 2% of the original 10^{-1} m pumice clasts exiting the vent. Owing to the form of the disruption probability, an even smaller percentage of pumice $>10^{-1}$ m would be expected to exit the conduit. Similar trends are observed in the Lagrangian analysis that gives statistics by tracing the path of individual particles (Fig. 4). For particles exiting the vent, almost all pumice clasts greater than a few centimetres in diameter have multiple disruptive collisions with the number increasing with greater fragmentation depths.

Both analytical and numerical treatments of granular disruption in conduits imply that some of the largest pumice clasts preserved in volcanic deposits are unlikely to have been generated during deep fragmentation events. This should be true for a range of pumice compositions, vesicularities and crystal contents as shown

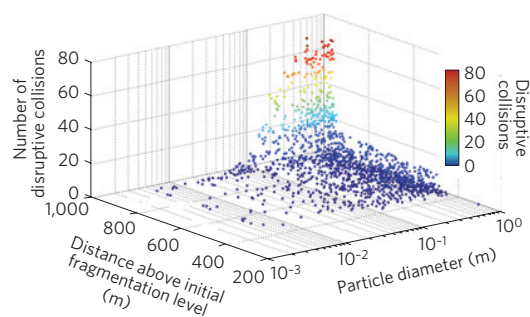


Figure 4 | Lagrangian analysis of disruptive collisions. Shown are the number of disruptive collisions a particle incurs as a function of particle diameter and distance above the fragmentation level. Large pumice produced from deep fragmentation levels endure multiple disruptive collisions and have the least chance of surviving intact.

by the limited variability in disruption thresholds for dense glass and sintered glass beads. Widening of the conduit can partially explain increases in grain size, but disruption is more sensitive to fragmentation depth given the limited variability in conduit diameter. Although there will always be a finite probability for large clasts to survive granular disruption as they transit the conduit, the observation of numerous large pumice clasts in a deposit provides a depositional record that fragmentation was shallow, at least transiently. Such indicators are important owing to the difficulty of imaging the fragmentation level in contemporary events and the near impossibility of determining the fragmentation level of pre-geophysically instrumented eruptions. Past events that include some of the largest volcanic eruptions, so-called super volcanoes, have never been witnessed so indications of their fragmentation level provide important clues to their eruptive dynamics²⁴.

The absence of large pumice does not require deep fragmentation, as efficient primary fragmentation cannot be ruled out. However granular disruption may confound interpretation of the initial fragmentation mechanism except in cases of shallow fragmentation. Deep fragmentation events will on average produce finer mixtures of particles resulting in slower mixtures at the vent owing to choked flow conditions. In general this will make these

eruption columns more likely to collapse than would be expected if comminution did not occur in the conduit^{9,25,26}. Hence fragmentation depth, through the mechanism of granular disruption, may exhibit a first-order control on the style of an eruption by determining whether it produces a buoyant plume ascending into the stratosphere or a ground-hugging pyroclastic flow inundating the surrounding countryside.

Methods

Experiments. We carried out a series of experiments on volcanic clasts during short-duration collisions. We used rhyolite pumice from tephra fall deposits of Medicine Lake Volcano in northern California. Average clast density is $550 \pm 39 \text{ kg m}^{-3}$, bubble size mode smaller than 1 mm (ref. 27) and particle mass was $0.145\text{--}0.881 \pm 0.001 \text{ g}$. Pumice particles were propelled by compressed nitrogen (2,000 fps) and mass was measured before and after each experiment. Disruption rate was insensitive to the macroscopic impact angle as the particle roughness created a random impact angle for the first point of contact on the microscale. The particles generated in disruptive collisions are angular and using two-dimensional proxies for particle roundness¹⁵, collections of these particles are indistinguishable from the angularity of the initial fall deposit pumice.

When a collision produces a fragment larger than an arbitrary 25% of the original size, we refer to it as a disruptive collision. Although the specific threshold used is arbitrary, the calculations using this parameter are relatively insensitive to other choices as the transition in style of fragmentation is abrupt.

We examined the potential for agglutination of discrete silic magmatic particles under these conduit conditions. However, agglutination at collisional energies in the conduit is unlikely (coalescence typically occurs at energies of less than 10^{-6} mJ , more than six orders of magnitude less than the collisions considered here^{28,29}). Although post-fragmentation material in volcanic conduits remains hot and will deform over long timescales, viscous deformation during these high-velocity impacts is minimal⁷. Even over the duration of flight from initial fragmentation to exiting the conduit the particles retain angular shapes as observed in fall deposits.

Numerical simulations. Only the region in the conduit above the fragmentation level is modelled. We fix the initial particle volume fraction (0.30) and initial pressure (lithostatic pressure assuming a crustal density of $2,700 \text{ kg m}^{-3}$). The exit pressure was fixed at atmospheric pressure. A small expansion region (100 m) above the conduit exit was also modelled to create a choked flow region. Although we do not explicitly fix the velocity at the vent to a choked flow velocity the instantaneous average velocity at the vent varied less than $\sim 10\%$ from isothermal dusty gas approximations with velocity fluctuations in time being highly correlated with the local volume fraction of particles. The small deviation from the dusty gas speed of sound is due to the slip velocity between the large particles and the gas phase. The fragmentation depth was varied from 0.5 to 3.0 km. Conduit width was held constant at 50 m and the spatial resolution of all simulations was 2 m. We have explored a range of restitution coefficients that account for the energy lost during inelastic collisions. The general behaviour is similar across a range of restitution coefficients; here we use a restitution coefficient of 0.5 based on our experimental measurements¹⁰. For comparison, all simulations are run in two modes, one including the effect of disruptive collisions and the other neglecting disruption. In the numerical simulations, separate conservation equations represent different size clasts coupled through drag terms (Supplementary Methods). Hence the residence time of particles and Stokes number behaviour (particle inertia) differs from the simplified residence time assumptions in the analytical calculations.

Received 1 February 2012; accepted 19 June 2012; published online 22 July 2012

References

1. Wohletz, K. H., Sheridan, M. F. & Brown, W. K. Particle-size distributions and the sequential fragmentation-theory applied to volcanic ash. *J. Geophys. Res.* **94**, 15703–15721 (1989).
2. Buttner, R., Dellino, P., Raue, H., Sonder, I. & Zimanowski, B. Stress-induced brittle fragmentation of magmatic melts: Theory and experiments. *J. Geophys. Res.* **111**, B08204 (2006).
3. Heiken, G. Morphology and petrography of volcanic ashes. *Geol. Soc. Am. Bull.* **83**, 1961–1988 (1972).
4. Kueppers, U., Scheu, B., Spieler, O. & Dingwell, D. B. Fragmentation efficiency of explosive volcanic eruptions: A study of experimentally generated pyroclasts. *J. Volcanol. Geotherm. Res.* **153**, 125–135 (2006).
5. Zhang, Y. X. A criteria for the fragmentation of bubbly magma based on brittle failure theory. *Nature* **402**, 648–650 (1999).
6. Papale, P. Strain-induced magma fragmentation in explosive eruptions. *Nature* **397**, 425–428 (1999).
7. Dingwell, D. B. Volcanic dilemma: Flow or blow? *Science* **273**, 1054–1055 (1996).
8. Sparks, R. S. J. The dynamics of bubble deformation and growth in magmas: A review and analysis. *J. Volcanol. Geotherm. Res.* **3**, 1–37 (1978).
9. Papale, P. Dynamics of magma flow in volcanic conduits with variable fragmentation efficiency and nonequilibrium pumice degassing. *J. Geophys. Res.* **106**, 11043065–1111065 (2001).
10. Dufek, J. & Manga, M. *In situ* production of ash in pyroclastic flows. *J. Geophys. Res.* **113**, B09207 (2008).
11. Schwarzkopf, L. M., Spieler, O., Scheu, B. & Dingwell, D. B. Fall-experiments on Merapi basaltic andesite and constraints on the generation of pyroclastic surges. *eEarth* **2**, 1–5 (2007).
12. Walker, G. P. L. Generation and dispersal of fine ash and dust by volcanic eruptions. *J. Volcanol. Geotherm. Res.* **11**, 81–92 (1981).
13. Setoh, M. *et al.* High- and low-velocity impact experiments on porous sintered glass bead targets of different compressive strengths: Outcome sensitivity and scaling. *Icarus* **205**, 702–711 (2010).
14. Evans, J. R., Huntoon, J. E., Rose, W. I., Varley, N. R. & Stevenson, J. A. Particle sizes of andesitic ash fallout from vertical eruptions and co-pyroclastic flow clouds, Volcan de Colima, Mexico. *Geology* **37**, 935–938 (2009).
15. Manga, M., Patel, A. & Dufek, J. Rounding of pumice clasts during transport: Field measurements and laboratory studies. *Bull. Volcanol.* **73**, 321–333 (2011).
16. Taddeucci, J. & Palladino, D. M. Particle size–density relationships in pyroclastic deposits: Inferences for emplacement processes. *Bull. Volcanol.* **64**, 273–284 (2002).
17. Darteville, S. & Valentine, G. A. Transient multiphase processes during the explosive eruption of basalt through a geothermal borehole (Namafjall, Iceland, 1977) and implications for natural volcanic flows. *Earth Planet. Sci. Lett.* **262**, 363–384 (2007).
18. Kaminski, E. & Jaupart, C. The size distribution of pyroclasts and the fragmentation sequence in explosive volcanic eruptions. *J. Geophys. Res.* **103**, 29759–29779 (1998).
19. Papale, P. Dynamics of magma flow in volcanic conduits with variable fragmentation efficiency and nonequilibrium pumice degassing. *J. Geophys. Res.* **106**, 11043–11065 (2001).
20. Dobran, F. Nonequilibrium flow in volcanic conduits and application to the eruptions of Mt. St. Helens on May 18, 1980, and Vesuvius in AD 79. *J. Volcanol. Geotherm. Res.* **49**, 285–311 (1992).
21. Dufek, J. D. & Bergantz, G. W. Transient two-dimensional dynamics in the upper conduit of a rhyolitic eruption: A comparison of the closure models for the granular stress. *J. Volcanol. Geotherm. Res.* **143**, 113–132 (2005).
22. Syamlal, M., Rogers, W. & O'Brien, T. J. *MFIX Theory Guide* Technical Note, 1–49 (US Department of Energy, Morgantown, WV, 1993).
23. Dufek, J., Wexler, J. & Manga, M. Transport capacity of pyroclastic density currents: Experiments and models of substrate–flow interaction. *J. Geophys. Res.* **114**, B11203 (2009).
24. Legros, F. & Kelfoun, K. Sustained blasts during large volcanic eruptions. *Geology* **28**, 895–898 (2000).
25. Neri, A., Di Muro, A. & Rosi, M. Mass partition during collapsing and transitional columns by using numerical simulations. *J. Volcanol. Geotherm. Res.* **115**, 1–18 (2002).
26. Darteville, S., Rose, W. I., Stix, J., Kelfoun, K. & Vallance, J. W. Numerical modeling of geophysical granular flows: 2. Computer simulations of plinian clouds and pyroclastic flows and surges. *Geochem. Geophys. Geosyst.* **5**, 1–36 (2004).
27. Cagnoli, B. & Manga, M. Granular mass flows and Coulomb's friction in shear cell experiments: Implications for geophysical flows. *J. Geophys. Res.* **109**, F04005 (2004).
28. Low, T. B. & List, R. Collision, coalescence and breakup of raindrops. Part I: Experimentally established coalescence efficiencies and fragment size distributions in breakup. *J. Atmos. Sci.* **39**, 1591–1606 (1982).
29. Telling, J. & Dufek, J. An experimental evaluation of ash aggregation in explosive volcanic eruptions. *J. Volcanol. Geotherm. Res.* **209–210**, 1–8 (2012).
30. Gault, D. E. & Wedekind, J. A. The destruction of tectites by micrometeoroid impact. *J. Geophys. Res.* **74**, 6780–6794 (1969).

Acknowledgements

This work was supported by NSF grants 0809321 (J.D.) and 0809564 (M.M.). We thank K. Russell for comments on this manuscript.

Author contributions

J.D. developed the analysis and numerical model and A.P. and M.M. carried out most of the experiments. All authors contributed to the ideas presented in the manuscript.

Additional information

Supplementary information is available in the online version of the paper. Reprints and permissions information is available online at www.nature.com/reprints. Correspondence and requests for materials should be addressed to J.D.

Competing financial interests

The authors declare no competing financial interests.